Journal of Computational Mathematics
Vol.37, No.5, 2019, 720–737.

http://www.global-sci.org/jcm
doi:10.4208/jcm.1809-m2016-0761

THE DESIGN OF BÉZIER SURFACE THROUGH QUINTIC BÉZIER ASYMPTOTIC QUADRILATERAL*

Hui Wang and Chungang Zhu[1)]
School of Mathematical Sciences, Dalian University of Technology, Dalian 116024, China
Email: huiwang@mail.dlut.edu.cn, cgzhu@dlut.edu.cn
Caiyun Li
School of Mathematical and Physical Sciences, Dalian University of Technology, Panjin 124221, China
Email: caiyun@dlut.edu.cn

Abstract

The asymptotic curve is widely used in astronomy, mechanics and numerical optimization. Moreover, it shows great application potentials in architecture. We focus on the problem how to cover bounded asymptotic curves by a freeform surface. The paper presents the necessary and sufficient conditions for quadrilateral with non-inflection being asymptotic boundary curves of a surface. And then, with given corner data, we model quintic Bézier asymptotic quadrilateral interpolated by a smooth Bézier surface of bi-eleven degree. We handle the available degrees of freedom during the construction to get an optimized result. Some representative surfaces bounded by asymptotic curves with lines or inflections are also discussed by examples. The presented interpolation scheme for the construction of tensor-product Bézier surfaces is compatible with the CAD systems.

Mathematics subject classification: 65D07.
Key words: Asymptotic curves, Bézier surface, Interpolation, Quadrilateral.

1. Introduction

The curve's asymptotic direction is a direction along which the normal curvature is zero. If the tangent vector $\mathbf{e}$ at each point of the curve $\mathbf{r}$ on a surface $\mathbf{R}(u, v)$ is an asymptotic direction of the surface $\mathbf{R}(u, v)$, then the curve is an asymptotic curve of the surface. Asymptotes have been applied in many areas, such as astronomy [1], mechanics [2], numerical optimization [3], architecture [4] and relevant subjects.

Architectural geometry [5] addresses challenges in the realization of complex freeform structures and technical advantages of ruled surfaces. A typical example is hyperbolic paraboloids with negative Gaussian curvatures. Moreover, asymptotic curves can only exist on this kind of negatively curved surface and there are two asymptotic directions at each point of the anticlastic surface-regions. Based on the analysis of these asymptotic curves, this locally saddle-shaped regions can be approximated by ruled surface. Flöry and Pottmann [4] just used asymptotic directions, which were estimated from the given point cloud, to deduce the layout of production sized panels and construct an initial ruled surface by aligning rulings with asymptotic curves.

However, except analyzing the asymptotic curves or interpolating some points as the asymptotic boundary by large ruled surface patches or multiple strips of ruled surfaces, if there exists other general surfaces in practical application?

* Received October 8, 2016 / Revised version received June 7, 2018 / Accepted September 12, 2018 / Published online January 30, 2019 /
[1)] Corresponding author

In fact, since asymptotic curves are the only type to combine the benefits of straight unrolling and orthogonal nodes along a double-curved grid, they show great application potentials in architectural design. A remarkable realization of this structure is provided by 'Asymptotic Gridshell', which was developed by Eike Schling and Denis Hitrec at TU Munich (see Fig. 1.1 or website https://www.lt.ar.tum.de/en/research-pavilion/ in detail). They designed developable curved support structures along asymptotic parameter lines and orientated normal to minimal surface [6]. Recent work in [7] generalizes above structure to discretization of asymptotic nets with constant ratio of principle curvatures. The definition of discrete asymptotic net comes from discrete A-net in discrete differential geometry [8]. Also based on this asymptotic gridshell structure, [9] uses a special network to discretize a surface of constant mean curvatures, which shows that when the network becomes an asymptotic one, the surface is a minimal surface. In above freeform structure, beams are asymptotic curves lying on the underlying surface and together with the developable lamelles show good aesthetic qualities. The coverage of a freeform surface is also a main problem in architectural geometry. If we fill in the gridshell by the underlying surface patches, then each patch of the grid is bounded by asymptotic curves of itself. This locally inverse reconstruction problem motives our interest. Then it comes to a basic geometric problem that how to construct a surface possessing the given curves as its asymptotic boundary curves.

Fig. 1.1. 'Asymptotic Gridshell' forms the INSIDE\OUT pavilion. (Picture: Hui Wang)

The study on reconstruction of smooth surfaces from a given boundary curve is a hot topic. Many researchers studied on the construction of surfaces interpolating the special curves, but most of which are geodesics and lines of curvature. Wang et al. [10] constructed parametric surfaces which possess a given spatial curve as a geodesic, and Li et al. constrained a line of curvature as the boundary curve of the surfaces [11]. Kasap et al. [12] and Li et al. [13] extended the parametric surfaces into a generalization of surface family interpolating a geodesic curve and a line of curvature, respectively. Li et al. also designed developable surfaces through Bézier geodesics [14] and a given line of curvature [15]. The number of given curves of these constructed surfaces are at most two. However, Farouki et al. gave the sufficient and necessary conditions of closed geodesic curves [16] and lines of curvature [17] as boundary curves of Coons quadrilateral patches. Based on the conditions in [16], he constructed triangular Coons patches [18] with geodesic boundary curves and four-sided Bézier patches [19] with Bézier curves as geodesic

boundaries. In order to overcome the high degree of the constructed surfaces in [19], Yang and Wang constructed a tensor-product Bézier surface [20] and B-spline surface [21] of lower degrees through Bézier and B-spline geodesic quadrilateral, respectively.

Constructing a surface from given asymptotic curves has not been widely studied. Inspired by the applications in architectural design, Bayram et al. [22] extended the method in [10] to construct a parametric surface pencil with an asymptote, Atalay et al. [23] identified a surfaces family with Cartan frame to interpolate an asymptote and so on. These interpolations are relevant to no more than two asymptotic curves and most surfaces are ruled surfaces.

From the mathematical perspective, we follow up on recent work [24, 25] about B-spline and rational Bézier surface interpolating the closed asymptotic boundaries and are interested in the generalization to Bézier surface. Motivated by the potential application in architecture [4, 6, 7, 9], we analyze the local property for one patch of surface bounded by asymptotic boundaries. We optimize the quadrilaterals and smooth the interpolated surfaces by minimizing the strain energy and thin plate spline energy. In order to be compatible with the requirements of the commercial CAD systems, we design the tensor product Bézier surface through Bézier asymptotic quadrilateral.

The paper is arranged as follows. Section 2 recalls some basic facts from differential geometry and identifies the condition for a non-linear regular curve to be an asymptote on the surface. Section 3 proposes the identification of four curves free of inflections being asymptotic boundaries of a surface, based on which we construct an optimized Bézier asymptotic quadrilateral by minimizing the strain energy with given corner data of a quintic quadrilateral. Then Section 4 satisfies the global boundary constraints to interpolate this asymptotic quadrilateral and constructs a smooth tensor-product Bézier surface of bi-eleven degree by minimizing the thin plate spline energy. Surfaces interpolating boundary quadrilateral including lines and inflections are also discussed by some examples together with degree explanation of constructed structure in Section 5. At last, Section 6 concludes the whole paper and poses further work.

2. Preliminaries

A curve is regular if it admits a tangent line at each point of it. In the following discussions all curves are assumed to be regular. In this paper, $\dot{\mathbf{r}}(s)$ and $\mathbf{r}'(t)$ denote the derivatives of $\mathbf{r}$ with respect to arc-length parameter s and arbitrary parameter t, respectively. Let us briefly review some basic facts about Frenet and Darboux frames from differential geometry ([26]).

For a point $\mathbf{r}(s)$ of a space curve satisfying $\ddot{\mathbf{r}}(s) \neq 0$, we denote its Serret-Frenet frame is ($\mathbf{e}(s)$,$\mathbf{n}(s)$,$\mathbf{b}(s)$), where $\mathbf{e}(s)$,$\mathbf{n}(s)$ and $\mathbf{b}(s)$ are respectively called the unit tangent, principal normal and binormal vector of the curve at the point $\mathbf{r}(s)$. Darboux frame ($\mathbf{e}(s)$,$\mathbf{h}(s)$,$\mathbf{N}(s)$) is attached to space curve $\mathbf{r}(s) = \mathbf{R}(u(s), v(s))$ on surface $\mathbf{R}(u, v)$, where $\mathbf{e}(s)$ is still the unit tangent vector of the curve, $\mathbf{N}(s) = \frac{\mathbf{R}_u(u,v)\times\mathbf{R}_v(u,v)}{||\mathbf{R}_u(u,v)\times\mathbf{R}_v(u,v)||}$ is the unit normal vector of the surface, and $\mathbf{h}(s) = \mathbf{N}(s) \times \mathbf{e}(s)$ at the point $\mathbf{R}(u(s), v(s)) = \mathbf{r}(s)$.

Given the general parametric curve $\mathbf{r}$: $t \to \mathbf{r}(t)$, we have the similar definition of its Serret-Frenet and Darboux frame as defined above with arc-length parameterization.

Lemma 2.1 ([26]). *A curve on the surface is an asymptotic curve if and only if it is a line or its osculating plane is its tangent plane.*

Apart from the condition that $\mathbf{r}$ is a line, if $\mathbf{r}$ on the surface $\mathbf{R}(u, v)$ is an asymptotic curve, the curve's normal curvature k_n is identically zero. Since the curvature k, the normal

curvature k_n and the geodesic curvature k_g satisfy $k^2 = k_g^2 + k_n^2$, then $k = \sigma k_g$, $\sigma = \pm 1$. From the Serret-Frenet and Darboux frames relations, we get $\mathbf{h} = \sigma\mathbf{n}$ and $\mathbf{N} = \sigma\mathbf{b}$ for both arc-length parameter and general parameter. Therefore, the Frenet and Darboux frames agree modulo signs for both kinds of parameters. Consequently, we have the following conditions which identify an asymptotic curve on a surface for a general parameter.

Lemma 2.2. *A non-linear regular curve $\boldsymbol{r}(t)$ without inflections is an asymptotic on the surface $\boldsymbol{R}(u, v)$ if and only if it satisfies the following conditions and all these conditions are equivalent to one another*

- *the normal curvature of $\boldsymbol{r}(t)$ is identical zero;*
- *the binormal at each non-inflection point of $\boldsymbol{r}(t)$ is orthogonal to the surface tangent plane at the point $\boldsymbol{R}(u(t), v(t)) = \boldsymbol{r}(t)$;*
- *the rectifying plane at each non-inflection point of $\boldsymbol{r}(t)$ is orthogonal to the surface tangent plane at the point $\boldsymbol{R}(u(t), v(t)) = \boldsymbol{r}(t)$.*

Remark 2.1. Above analysis need the existence of binormal vector of regular curve, which means $\mathbf{r}''(t) \neq 0$. When $\mathbf{r}''(t_0) = 0$ for some parameter t_0, $\mathbf{r}(t_0)$ is an inflection of the curve $\mathbf{r}(t)$ such that the curvature $k(t_0) = 0$, in which case there is no solution to the interpolation at such point. Therefore, the following construction builds on the analysis of non-inflection points of the boundary curves, and the curves are assumed to be non-linear. The case that boundary curves may be linear or have inflections will be discussed by examples in Section 5.1 and 5.2.

The goal of our paper is to construct a surface interpolating a quadrilateral, which is built from the given data, as its asymptotic boundaries. Such boundary quadrilateral is called asymptotic quadrilateral. In order to realize this goal, we need to analyze the local corner conditions and global boundary compatibility for the boundary to be asymptotic curves of the supposed interpolating surface. There are two steps to achieve our goal. Firstly, we need to give the conditions of being asymptotic quadrilateral and apply it to construct boundary quadrilateral being the crossing asymptotes under the local corner conditions on a surface (in Section 3). Secondly, a surface is modeled to interpolate this quadrilateral under global boundary compatible condition (in Section 4).

3. Quintic Bézier Asymptotic Quadrilateral

In this section, we aim to construct the quadrilateral satisfying the constraints of the crossing asymptotes on a surface. At first, we analyze the conditions of two asymptotic curves crossing on the same surface and generalize it to the constraints for asymptotic quadrilateral. More precisely, we construct quintic Bézier asymptotic quadrilateral and optimize it by minimizing the strain energy.

3.1. Conditions of asymptotic curves crossing on the same surface

Lemma 3.1. *Consider an arc-length parametric regular curve $\boldsymbol{r}(s)$ on a surface $\boldsymbol{R}(u, v)$, setting $\boldsymbol{N}(s) = \sigma\boldsymbol{b}(s)$ with $\sigma = \pm 1$, we have $\boldsymbol{h}(s) = \sigma\boldsymbol{n}(s)$, $k_n(s) = 0$, $k(s) = \sigma k_g(s)$, $\tau_g(s) = -\tau(s)$, where $\tau_g(s)$ and $\tau(s)$ are the geodesic torsion and torsion.*

Proof. $\mathbf{N}(s) = \sigma\mathbf{b}(s)$ directly leads to $\mathbf{h}(s) = \sigma\mathbf{n}(s)$, which means that the Frenet and Darboux frames agree modulo signs. From the Serret-Frenet frame relation, we have the following equations:

$$\begin{aligned}
\begin{pmatrix} \dot{\mathbf{e}}(s) \\ \dot{\mathbf{h}}(s) \\ \dot{\mathbf{N}}(s) \end{pmatrix} &= \begin{pmatrix} \dot{\mathbf{e}}(s) \\ \sigma\dot{\mathbf{n}}(s) \\ \sigma\dot{\mathbf{b}}(s) \end{pmatrix} = \begin{pmatrix} 1 & 0 & 0 \\ 0 & \sigma & 0 \\ 0 & 0 & \sigma \end{pmatrix} \begin{pmatrix} 0 & k(s) & 0 \\ -k(s) & 0 & \tau(s) \\ 0 & -\tau(s) & 0 \end{pmatrix} \begin{pmatrix} \mathbf{e}(s) \\ \mathbf{n}(s) \\ \mathbf{b}(s) \end{pmatrix} \\
&= \begin{pmatrix} 0 & k(s) & 0 \\ -\sigma k(s) & 0 & \sigma\tau(s) \\ 0 & -\sigma\tau(s) & 0 \end{pmatrix} \begin{pmatrix} \mathbf{e}(s) \\ \mathbf{n}(s) \\ \mathbf{b}(s) \end{pmatrix} \\
&= \begin{pmatrix} 0 & k(s) & 0 \\ -\sigma k(s) & 0 & \sigma\tau(s) \\ 0 & -\sigma\tau(s) & 0 \end{pmatrix} \begin{pmatrix} 1 & 0 & 0 \\ 0 & \sigma & 0 \\ 0 & 0 & \sigma \end{pmatrix} \begin{pmatrix} \mathbf{e}(s) \\ \mathbf{h}(s) \\ \mathbf{N}(s) \end{pmatrix} \\
&= \begin{pmatrix} 0 & \sigma k(s) & 0 \\ -\sigma k(s) & 0 & \tau(s) \\ 0 & -\tau(s) & 0 \end{pmatrix} \begin{pmatrix} \mathbf{e}(s) \\ \mathbf{h}(s) \\ \mathbf{N}(s) \end{pmatrix}.
\end{aligned}$$

Compared with the Darboux frame relation, we get $k_n(s) = 0$, $k(s) = \sigma k_g(s)$, $\tau_g(s) = -\tau(s)$. This completes the proof of the lemma. □

Proposition 3.1. *If two different arc-length parametric asymptotic curves $\boldsymbol{r}_1(s)$ and $\boldsymbol{r}_2(s)$ on the same surface $\boldsymbol{R}(u, v)$ crossing at a non-inflection point $\boldsymbol{P} = \boldsymbol{r}_1(s_1) = \boldsymbol{r}_2(s_2)$ satisfy $\boldsymbol{N}_P = \sigma_1\boldsymbol{b}_1(s_1) = \sigma_2\boldsymbol{b}_2(s_2)$ with σ_1, $\sigma_2 = \pm 1$, then*

$$\tau_1(s_1) = -\tau_2(s_2),$$

where $\boldsymbol{N}_P$ is the surface normal, $\boldsymbol{b}_1(s_1)$, $\tau_1(s_1)$ and $\boldsymbol{b}_2(s_2)$, $\tau_2(s_2)$ are respectively the binormal vectors and torsions of $\boldsymbol{r}_1(s_1)$ and $\boldsymbol{r}_2(s_2)$ at the point $\boldsymbol{P}$.

Proof. For two different asymptotic curves $\mathbf{r}_1(s)$ and $\mathbf{r}_2(s)$ on the same surface $\mathbf{R}(u, v)$, their normal curvatures are $k_{n1}(s) = 0$, $k_{n2}(s) = 0$, then $\mathbf{N}_1(s) = \sigma_1\mathbf{b}_1(s)$, $\mathbf{N}_2(s) = \sigma_2\mathbf{b}_2(s)$, respectively. From Lemma 3.1, we have $\tau_{g1}(s) = -\tau_1(s)$ and $\tau_{g2}(s) = -\tau_2(s)$, where $\tau_{g1}(s)$, $\tau_{g2}(s)$ are the geodesic torsion of $\mathbf{r}_1(s)$ and $\mathbf{r}_2(s)$.

For two directions in the surface tangent plane Π_p specified by the angles α_1, and α_2, since the normal curvature k_{n1}, k_{n2} and the geodesic torsion τ_{g1}, τ_{g2} satisfy $\sin(\alpha_2 - \alpha_1)[\tau_{g1}(\alpha_1) + \tau_{g2}(\alpha_2)] = \cos(\alpha_2 - \alpha_1)[k_{n1}(\alpha_1) - k_{n2}(\alpha_2)]$ (see, e.g., [10]), we have $\sin(\alpha_2 - \alpha_1)[\tau_{g1}(\alpha_1) + \tau_{g2}(\alpha_2)] = 0$. Since $\alpha = \alpha_2 - \alpha_1$ representing the oriented angle between the two curves $\mathbf{r}_1(s)$ and $\mathbf{r}_2(s)$ at $\mathbf{P}$ is nonvanishing, we have $\sin(\alpha_2 - \alpha_1) \neq 0$ which induces $\tau_1(s_1) = -\tau_2(s_2)$. □

Remark 3.1. Above analysis is based on the arc-length parameter of functions. For the general parameter of functions, we can have the same results. So we will discuss the general parametric curve next, and the parameters will be omitted when no confusion can rise.

Proposition 3.1 gives us the necessary condition of two curves which are crossing at one point being asymptotes. If we generalize the condition to quadrilateral formed by four curves, we can find that there are three constraints for quadrilateral being asymptotic to a surface. (The position relation of the four curves refers to Fig. 3.1).

Proposition 3.2. *Four curves* $\boldsymbol{r}_i(t)$ $(i = 1, \cdots, 4)$ *free of inflections are boundary asymptotes of a surface* $\boldsymbol{R}(u, v)$*, then these four curves satisfy the following three constraints:*

(C1) *rectifying constraints at corners: the binormal vectors* $\boldsymbol{b}_i(t)$ *of the four curves* $\boldsymbol{r}_i(t)$ *at four corners must agree modulo sign, that is*

$$\begin{aligned} \boldsymbol{N}_{12} &= \sigma_1(0)\boldsymbol{b}_1(0) = \sigma_2(0)\boldsymbol{b}_2(0), \quad & \boldsymbol{N}_{14} &= \sigma_1(1)\boldsymbol{b}_1(1) = \sigma_4(0)\boldsymbol{b}_4(0), \\ \boldsymbol{N}_{23} &= \sigma_2(1)\boldsymbol{b}_2(1) = \sigma_3(0)\boldsymbol{b}_3(0), \quad & \boldsymbol{N}_{34} &= \sigma_3(1)\boldsymbol{b}_3(1) = \sigma_4(1)\boldsymbol{b}_4(1), \end{aligned} \tag{3.1}$$

where $\boldsymbol{N}_{12}$, $\boldsymbol{N}_{14}$, $\boldsymbol{N}_{23}$, $\boldsymbol{N}_{34}$ *are unit normal vectors of the surface at four corners, and* $\sigma_i(j) = \pm 1$ *(*$i = 1, \cdots, 4$, $j = 0, 1$*).*

(C2) *asymptotic crossing constraints at corners:*

$$\tau_1(0) = -\tau_2(0), \quad \tau_1(1) = -\tau_4(0), \quad \tau_2(1) = -\tau_3(0), \quad \tau_3(1) = -\tau_4(1). \tag{3.2}$$

(C3) *normal orientation constraints along boundaries: normal vectors along boundaries* $\boldsymbol{N}_i(t)$ *are continuous and satisfy* $\boldsymbol{N}_i(t) = \pm\boldsymbol{b}_i(t)$ *(*$i = 1, \cdots, 4$*).*

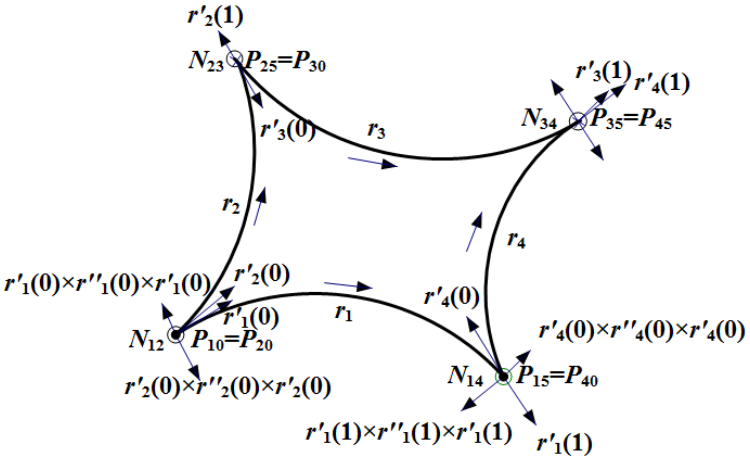

Fig. 3.1. Quadrilateral with vectors at four corners.

Boundaries being asymptotic to a surface is only related with boundary constraints. Above three constraints are necessary. Conversely, if any of these three conditions is not satisfied, there will be no such surface interpolating the asymptotic quadrilateral. Therefore, these three constraints are the necessary and sufficient constraints to exist an interpolating surface.

From (3.1) and (3.2), it is easy to know that conditions (C1) and (C2) are local corner constraints. And condition (C3) is a global boundary condition compatible with the surface. In order to construct a surface whose boundary quadrilateral is asymptotic, (C1) and (C2) can help us construct the asymptotic quadrilateral firstly, then (C3) helps to construct an interpolating surface.

3.2. Constraints for quintic Bézier asymptotic quadrilateral

We hope to construct an optimized Bézier asymptotic quadrilateral by choosing some free parameters. A real world requirement of given corner positions, tangents and curvatures can be satisfied with the degree of curves being at least 5. Therefore, the following focuses on the

construction of quintic asymptotic quadrilateral. We assume that the four boundary curves free of inflections are quintic Bézier curves

$$\mathbf{r}_i(u) = \sum_{j=0}^{5} \mathbf{P}_{ij} B_j^5(u),\ (i = 1, 3)\ ,\ \mathbf{r}_i(v) = \sum_{j=0}^{5} \mathbf{P}_{ij} B_j^5(v), \quad (i = 2, 4),$$

with the given corner data including the corner vectors (as shown in Fig. 3.1)

$$\mathbf{r}_1(0) = \mathbf{P}_{10} = \mathbf{P}_{20} = \mathbf{r}_2(0),\ \mathbf{r}_1(1) = \mathbf{P}_{15} = \mathbf{P}_{40} = \mathbf{r}_4(0),$$

$$\mathbf{r}_2(1) = \mathbf{P}_{25} = \mathbf{P}_{30} = \mathbf{r}_3(0),\ \mathbf{r}_3(1) = \mathbf{P}_{35} = \mathbf{P}_{45} = \mathbf{r}_4(1),$$

$$\mathbf{P}_{11},\ \mathbf{P}_{14},\ \mathbf{P}_{21},\ \mathbf{P}_{24},\ \mathbf{P}_{31},\ \mathbf{P}_{34},\ \mathbf{P}_{41},\ \mathbf{P}_{44},$$

and curvatures $k_i(j)$ $(i = 1, \cdots, 4,\ j = 0, 1)$. Then the eight points $\mathbf{P}_{12}$, $\mathbf{P}_{13}$, $\mathbf{P}_{22}$, $\mathbf{P}_{23}$, $\mathbf{P}_{32}$, $\mathbf{P}_{33}$, $\mathbf{P}_{42}$, $\mathbf{P}_{43}$ are unknown and need to be determined.

Remark 3.2. Above given corner data for the quintic Bézier curves are prerequisites and arbitrary. From the following solution, we find that there are four free parameters left. Then we can get optimized result by choosing those parameters properly. Moreover, the quintic Bézier quadrilateral can be replaced by curves of higher degrees for more than four free parameters left, and the method is working, too.

Given four Bézier curves free of inflections, we hope to construct a Bézier patch that interpolates these curves as asymptotic boundaries. The Proposition 3.2 offers three constraints and gives the identification of asymptotic quadrilateral. The following solves the unknown control points of the quintic Bézier quadrilateral under these three constraints.

(a) Rectifying constraints at corners.

Consider the rectifying constraints (3.1) and take the corner point $\mathbf{P}_{10}$ for example. Since the unit normal vector $\mathbf{N}_{12} = \frac{\mathbf{r}_1'(0)\times\mathbf{r}_2'(0)}{||\mathbf{r}_1'(0)\times\mathbf{r}_2'(0)||}$ of the surface is parallel to unit binormal vectors $\mathbf{b}_1(0) = \frac{\mathbf{r}_1'(0)\times\mathbf{r}_1''(0)}{||\mathbf{r}_1'(0)\times\mathbf{r}_1''(0)||}$ and $\mathbf{b}_2(0) = \frac{\mathbf{r}_2'(0)\times\mathbf{r}_2''(0)}{||\mathbf{r}_2'(0)\times\mathbf{r}_2''(0)||}$, then both $\mathbf{r}_1''(0)$ and $\mathbf{r}_2''(0)$ are located in the tangent plane Π_{12} of the surface at the point $\mathbf{P}_{10}$. Namely, points $\mathbf{P}_{10}$, $\mathbf{P}_{11}$, $\mathbf{P}_{12}$, $\mathbf{P}_{21}$, $\mathbf{P}_{22}$ are in the same plane such that $\mathbf{P}_{12}$ and $\mathbf{P}_{22}$ can be written as

$$\mathbf{P}_{12} = \mathbf{P}_{10} + \lambda_{12}(\mathbf{P}_{11} - \mathbf{P}_{10}) + \mu_{12}(\mathbf{P}_{21} - \mathbf{P}_{20}),$$
$$\mathbf{P}_{22} = \mathbf{P}_{20} + \lambda_{22}(\mathbf{P}_{11} - \mathbf{P}_{10}) + \mu_{22}(\mathbf{P}_{21} - \mathbf{P}_{20}),$$

where λ_{12}, μ_{12}, λ_{22}, μ_{22} are real. For the other three corner points, we can assume the similar representation:

$$\mathbf{P}_{32} = \mathbf{P}_{30} + \lambda_{32}(\mathbf{P}_{24} - \mathbf{P}_{25}) + \mu_{32}(\mathbf{P}_{31} - \mathbf{P}_{30}),$$
$$\mathbf{P}_{23} = \mathbf{P}_{25} + \lambda_{23}(\mathbf{P}_{24} - \mathbf{P}_{25}) + \mu_{23}(\mathbf{P}_{31} - \mathbf{P}_{30}),$$
$$\mathbf{P}_{13} = \mathbf{P}_{15} + \lambda_{13}(\mathbf{P}_{41} - \mathbf{P}_{40}) + \mu_{13}(\mathbf{P}_{14} - \mathbf{P}_{15}),$$
$$\mathbf{P}_{42} = \mathbf{P}_{40} + \lambda_{42}(\mathbf{P}_{41} - \mathbf{P}_{40}) + \mu_{42}(\mathbf{P}_{14} - \mathbf{P}_{15}),$$
$$\mathbf{P}_{33} = \mathbf{P}_{35} + \lambda_{33}(\mathbf{P}_{34} - \mathbf{P}_{35}) + \mu_{33}(\mathbf{P}_{44} - \mathbf{P}_{45}),$$
$$\mathbf{P}_{43} = \mathbf{P}_{45} + \lambda_{43}(\mathbf{P}_{34} - \mathbf{P}_{35}) + \mu_{43}(\mathbf{P}_{44} - \mathbf{P}_{45}),$$

where λ_{32}, μ_{32}, λ_{23}, μ_{23}, λ_{13}, μ_{13}, λ_{42}, μ_{42}, λ_{33}, μ_{33}, λ_{43}, μ_{43} are real.

Using the curvature expression, we have

$$k_1(0) = \frac{4||(\mathbf{P}_{11} - \mathbf{P}_{10}) \times (\mathbf{P}_{12} - \mathbf{P}_{10})||}{5||\mathbf{P}_{11} - \mathbf{P}_{10}||^3},$$

which is an equation only about μ_{12}, so that we can get the value of μ_{12}. From the other seven curvature equations at the corners, we can deduce the values of λ_{13}, λ_{22}, μ_{23}, λ_{32}, μ_{33}, λ_{43}, μ_{42} in the same way.

(b) Asymptotic crossing constraints at corners.

The torsions at the four corners should satisfy the constraints (3.2). Due to the torsion expression, we have

$$\frac{det(\mathbf{P}_{11} - \mathbf{P}_{10}, \mathbf{P}_{12} - \mathbf{P}_{10}, \mathbf{P}_{13} - \mathbf{P}_{10})}{||(\mathbf{P}_{11} - \mathbf{P}_{10}) \times (\mathbf{P}_{12} - \mathbf{P}_{10})||^2} = -\frac{det(\mathbf{P}_{21} - \mathbf{P}_{20}, \mathbf{P}_{22} - \mathbf{P}_{20}, \mathbf{P}_{23} - \mathbf{P}_{20})}{||(\mathbf{P}_{21} - \mathbf{P}_{20}) \times (\mathbf{P}_{22} - \mathbf{P}_{20})||^2},$$

$$\frac{det(\mathbf{P}_{15} - \mathbf{P}_{14}, \mathbf{P}_{13} - \mathbf{P}_{15}, \mathbf{P}_{15} - \mathbf{P}_{12})}{||(\mathbf{P}_{15} - \mathbf{P}_{14}) \times (\mathbf{P}_{13} - \mathbf{P}_{15})||^2} = -\frac{det(\mathbf{P}_{41} - \mathbf{P}_{40}, \mathbf{P}_{42} - \mathbf{P}_{40}, \mathbf{P}_{43} - \mathbf{P}_{40})}{||(\mathbf{P}_{41} - \mathbf{P}_{40}) \times (\mathbf{P}_{42} - \mathbf{P}_{40})||^2},$$

$$\frac{det(\mathbf{P}_{25} - \mathbf{P}_{24}, \mathbf{P}_{23} - \mathbf{P}_{25}, \mathbf{P}_{25} - \mathbf{P}_{22})}{||(\mathbf{P}_{25} - \mathbf{P}_{24}) \times (\mathbf{P}_{23} - \mathbf{P}_{25})||^2} = -\frac{det(\mathbf{P}_{31} - \mathbf{P}_{30}, \mathbf{P}_{32} - \mathbf{P}_{30}, \mathbf{P}_{33} - \mathbf{P}_{30})}{||(\mathbf{P}_{31} - \mathbf{P}_{30}) \times (\mathbf{P}_{32} - \mathbf{P}_{30})||^2},$$

$$\frac{det(\mathbf{P}_{35} - \mathbf{P}_{34}, \mathbf{P}_{33} - \mathbf{P}_{35}, \mathbf{P}_{35} - \mathbf{P}_{32})}{||(\mathbf{P}_{35} - \mathbf{P}_{34}) \times (\mathbf{P}_{33} - \mathbf{P}_{35})||^2} = -\frac{det(\mathbf{P}_{45} - \mathbf{P}_{44}, \mathbf{P}_{43} - \mathbf{P}_{45}, \mathbf{P}_{45} - \mathbf{P}_{42})}{||(\mathbf{P}_{45} - \mathbf{P}_{44}) \times (\mathbf{P}_{43} - \mathbf{P}_{45})||^2},$$

each of which is respectively with respect to two parameters (λ_{23}, μ_{13}), (λ_{33}, μ_{22}), (λ_{12}, μ_{43}) and (λ_{42}, μ_{32}). Solving these equations, we can get μ_{13}, μ_{22}, μ_{43}, μ_{32}, which are expressed by λ_{23}, λ_{33}, λ_{12}, λ_{42}, respectively.

(c) Normal orientation constraints along boundaries.

Along the regular curves $\mathbf{r}_i$, the unit normal $\mathbf{N}_i$ of the surface and binormal $\mathbf{b}_i(t)$ $(i = 1, \cdots, 4)$ are parallel and continuous, then the number of reversals at four corners is even. That is

$$\prod_{i,j} \sigma_i(j) = 1, \quad (i = 1, \cdots, 4,\ j = 0, 1). \tag{3.3}$$

The signs of $\sigma_i(j)$ $(i = 1, \cdots, 4,\ j = 0, 1)$ are chosen based on the equations in (3.1), which is compatible with constraint (3.3).

Remark 3.3. (3.3) is just a necessary condition of condition (C3) and it's still a local corner condition. Since condition (C3) is a global boundary condition and closely related with the surface construction which will be discussed in the next section, (3.3) can be used to construct the asymptotic quadrilateral.

Until now, the problem of solving the eight unknown points has been transferred into acquiring the values of four parameters λ_{23}, λ_{33}, λ_{12}, λ_{42}. Since these parameters are freely chosen, we can get a family of asymptotic quadrilaterals satisfying above constraints. By minimizing the strain energy

$$\int_0^1 (||\mathbf{r}_1''(u)||^2 + ||\mathbf{r}_3''(u)||^2)du + \int_0^1 (||\mathbf{r}_2''(v)||^2 + ||\mathbf{r}_4''(v)||^2)dv, \tag{3.4}$$

the value of λ_{23}, λ_{33}, λ_{12}, λ_{42} are obtained so that the eight unknown points $\mathbf{P}_{12}$, $\mathbf{P}_{13}$, $\mathbf{P}_{22}$, $\mathbf{P}_{23}$, $\mathbf{P}_{32}$, $\mathbf{P}_{33}$, $\mathbf{P}_{42}$, $\mathbf{P}_{43}$ are determined. Fig. 4.1-(a),(d) show two optimized asymptotic quadrilateral and their control polygon.

Remark 3.4. The strain energy is just a choice for us to find a smoother boundary quadrilateral. If the users are not satisfied with this choice or want to add other restraints from practical application, they can replace it with other optimization model.

4. Bézier Asymptotic Quadrilateral Interpolation

In the last section, we have constructed the boundary asymptotic quadrilateral satisfying the local corner constraints. Thus, if we combine this quadrilateral with global boundary condition, then we can construct a surface interpolating above asymptotic quadrilateral. The Proposition 3.2 identifies four curves $\mathbf{r}_i(t)$ free of inflections being boundary asymptotes of a surface $\mathbf{R}(u,v)$. $(C3)$ restricts normal vectors $\mathbf{N}_i(t)$ are continuous and parallel with the binormal vectors $\mathbf{b}_i(t)$ $(i=1,\cdots,4)$. Thus, the tangent plane $\Pi_i(t)$ along the boundary curves $\mathbf{r}_i(t)$ of the interpolated surface $\mathbf{R}(u,v)$ is determined by the surface normal vectors $\mathbf{N}_i(t)$, that is $\Pi_i(t)=[\mathbf{r}_i(t),\mathbf{r}_i'(t),\mathbf{r}_i'(t)\times\mathbf{r}_i''(t)\times\mathbf{r}_i'(t)]$.

The transverse tangent vectors $\mathbf{T}_i(t)$ $(i=1,\cdots,4)$ are defined along the boundary curves of the interpolated surface $\mathbf{R}(u,v)$ and used to represent constraint (C3) to produce the surface. They are defined as

$$\mathbf{T}_1(u)=\mathbf{R}_v(u,0),\quad \mathbf{T}_3(u)=\mathbf{R}_v(u,1),\quad \mathbf{T}_2(v)=\mathbf{R}_u(0,v),\quad \mathbf{T}_4(v)=\mathbf{R}_u(1,v).$$

Since they should lie in the tangent plane $\Pi_i(t)$ and be coplanar with $\mathbf{r}_i'(t)$ and $[\mathbf{r}_i'(t)\times\mathbf{r}_i''(t)]\times\mathbf{r}_i'(t)$, they can be expressed by them with scalar functions $x_i(t)$ and $y_i(t)$ $(i=1,\cdots,4)$. Namely,

$$\mathbf{T}_i(t)=x_i(t)\mathbf{r}_i'(t)+y_i(t)[\mathbf{r}_i'(t)\times\mathbf{r}_i''(t)]\times\mathbf{r}_i'(t),\quad t\in[0,1]. \tag{4.1}$$

For quintic Bézier curve $\mathbf{r}_i(t)$, the degrees of $\mathbf{r}_i'(t)$ and $[\mathbf{r}_i'(t)\times\mathbf{r}_i''(t)]\times\mathbf{r}_i'(t)$ are quartic and ten. In order to construct an interpolated surface with lower degree, we can choose $x_i(t)=\sum_{j=0}^{7}\alpha_{ij}B_j^7(t)$, $y_i(t)=\sum_{j=0}^{1}\beta_{ij}B_j^1(t)$, where the coefficients α_{ij} and β_{ij} are real and they will be identified in the following.

4.1. Identification of transverse tangent vectors

$\mathbf{T}_i(t)$ must satisfy the following conditions:

- Interpolation of the tangent vectors,

$$\begin{aligned}&\mathbf{T}_1(0)=\mathbf{r}_2'(0),\ \mathbf{T}_1(1)=\mathbf{r}_4'(0),\\ &\mathbf{T}_2(0)=\mathbf{r}_1'(0),\ \mathbf{T}_2(1)=\mathbf{r}_3'(0),\\ &\mathbf{T}_3(0)=\mathbf{r}_2'(1),\ \mathbf{T}_3(1)=\mathbf{r}_4'(1),\\ &\mathbf{T}_4(0)=\mathbf{r}_1'(1),\ \mathbf{T}_4(1)=\mathbf{r}_3'(1).\end{aligned}$$

Take the corner $\mathbf{P}_{10}$ for example. $\mathbf{T}_1(0)=\mathbf{r}_2'(0)$ is equivalent to

$$\alpha_{10}(\mathbf{P}_{11}-\mathbf{P}_{10})+20\beta_{10}[(\mathbf{P}_{11}-\mathbf{P}_{10})\times(\mathbf{P}_{12}-\mathbf{P}_{10})]\times(\mathbf{P}_{11}-\mathbf{P}_{10})=\mathbf{P}_{21}-\mathbf{P}_{20}.$$

Then α_{10} and β_{10} can be represented as

$$\begin{aligned}\alpha_{10}&=\frac{(\mathbf{P}_{11}-\mathbf{P}_{10})\cdot(\mathbf{P}_{21}-\mathbf{P}_{20})}{||\mathbf{P}_{11}-\mathbf{P}_{10}||^2},\\ \beta_{10}&=\frac{det((\mathbf{P}_{11}-\mathbf{P}_{10})\times(\mathbf{P}_{12}-\mathbf{P}_{10}),(\mathbf{P}_{11}-\mathbf{P}_{10}),(\mathbf{P}_{21}-\mathbf{P}_{20}))}{20||(\mathbf{P}_{11}-\mathbf{P}_{10})\times(\mathbf{P}_{12}-\mathbf{P}_{10})\times(\mathbf{P}_{11}-\mathbf{P}_{10})||^2}.\end{aligned}$$

The first and last coefficients of $x_i(t)$ and $y_i(t)$ $(i=1,\cdots,4)$ can be solved in this way.

- Compatibility of the twist vectors,

$$\begin{aligned}&\mathbf{T}_1'(0)=\mathbf{T}_2'(0)=\mathbf{R}_{u,v}(0,0),\\&\mathbf{T}_2'(1)=\mathbf{T}_3'(0)=\mathbf{R}_{u,v}(0,1),\\&\mathbf{T}_1'(1)=\mathbf{T}_4'(0)=\mathbf{R}_{u,v}(1,0),\\&\mathbf{T}_3'(1)=\mathbf{T}_4'(1)=\mathbf{R}_{u,v}(1,1).\end{aligned}\tag{4.2}$$

  Each equation in (4.2) admits two pairs of equations from corresponding coordinates. Thus we can get α_{i1} and α_{i6} $(i=1,\cdots,4)$.

  Moreover, let A_{12} be the angle between $\mathbf{r}_1'(0)$ and $\mathbf{r}_2'(0)$ at the corner $\mathbf{P}_{10}$, and project $\mathbf{T}_1'(0)$ and $\mathbf{T}_2'(0)$ on $\mathbf{N}_{12}$ to get

$$\begin{aligned}\mathbf{T}_1'(0)\cdot\mathbf{N}_{12}&=\tau_1(0)\,||\mathbf{r}_1'(0)||\,||\mathbf{r}_2'(0)||\sin A_{12}\\\mathbf{T}_2'(0)\cdot\mathbf{N}_{12}&=-\tau_2(0)\,||\mathbf{r}_1'(0)||\,||\mathbf{r}_2'(0)||\sin A_{12},\end{aligned}$$

  which satisfy $\tau_1(0)=-\tau_2(0)$. Other relations in constraint $(C2)$ hold naturally at the other corners in the same deduction.

Without loss of generality, we can set the residual $\alpha_{ij}=0$ $(i=1,\cdots,4,\ j=2,\cdots,5)$ such that $\mathbf{T}_i(t)$ $(i=1,\cdots,4)$ can be obtained.

4.2. Bézier surface construction

$\mathbf{T}_i(t)$ $(i=1,\cdots,4)$ are critical to construct the interpolating surface under the global boundary compatible condition. In order to construct a Bézier surface interpolating the four boundary Bézier curves, it's necessary to express $\mathbf{T}_i(t)$ in Bézier form.

Because the degree of $\mathbf{T}_i(t)$ is eleven, then

$$\mathbf{T}_i(t)=\sum_{k=0}^{11}(\mathbf{E}_k^i+\mathbf{F}_k^i)B_k^{11}(t),\quad i=1,\cdots,4,\tag{4.3}$$

where

$$\mathbf{E}_k^i=5\sum_{j=\max(0,k-4)}^{\min(7,k)}\frac{\binom{7}{j}\binom{4}{k-j}}{\binom{11}{k}}\alpha_{ij}\cdot\Delta\mathbf{P}_{i,k-j},\quad \mathbf{F}_k^i=\frac{k\beta_{i1}}{11}\mathbf{G}_{k-1}^i+(1-\frac{k}{11})\beta_{i0}\mathbf{G}_k^i,$$

$$\mathbf{G}_k^i=5\sum_{j=\max(0,k-4)}^{\min(6,k)}\frac{\binom{6}{j}\binom{4}{k-j}}{\binom{10}{k}}\mathbf{H}_j^i\cdot\Delta\mathbf{P}_{i,k-j},\quad \mathbf{H}_j^i=\frac{7}{7-j}(\mathbf{L}_j^i-\frac{j}{7}\mathbf{L}_{j-1}^i),$$

$$\mathbf{L}_k^i=100\sum_{j=\max(0,k-3)}^{\min(4,k)}\frac{\binom{4}{j}\binom{3}{k-j}}{\binom{7}{k}}\Delta\mathbf{P}_{i,j}\times\Delta^2\mathbf{P}_{i,k-j},\ \Delta\mathbf{P}_{i,j}=\mathbf{P}_{i,j+1}-\mathbf{P}_{i,j},$$

$\Delta^2\mathbf{P}_{i,j}=\Delta\mathbf{P}_{i,j+1}-\Delta\mathbf{P}_{i,j}$.

Thus the degree of the tensor-product Bézier surface $\mathbf{R}(u,v)$ is bi-eleven, that is

$$\mathbf{R}(u,v)=\sum_{i=0}^{11}\sum_{j=0}^{11}\mathbf{Q}_{i,j}B_i^{11}(u)B_j^{11}(v),\tag{4.4}$$

where $\mathbf{Q}_{i,j}$ $(i = 0, \cdots, 11,\ j = 0, \cdots, 11)$ are control points of the surface.

The outermost control points $\mathbf{Q}_{0,i}$, $\mathbf{Q}_{i,0}$, $\mathbf{Q}_{11,i}$, $\mathbf{Q}_{i,11}$ $(i = 0, \cdots, 11,)$ can be determined by the control points of boundary quadrilateral. Elevating the boundary quintic Bézier curve to the degree of eleven as

$$\mathbf{r}_i(t) = \sum_{j=0}^{11} \mathbf{M}_j^i B_j^{11}(t),$$

where $\mathbf{M}_j^i$ are acquired by the degree elevation formula of Bézier curve ([27]). Then

$$\mathbf{Q}_{0,i} = \mathbf{M}_i^1, \quad \mathbf{Q}_{i,0} = \mathbf{M}_i^2, \quad \mathbf{Q}_{11,i} = \mathbf{M}_i^3, \quad \mathbf{Q}_{i,11} = \mathbf{M}_i^4, \quad i = 0, \cdots, 11.$$

From (4.3) and (4.4), we can get $(i = 1, \cdots, 10)$

$$\begin{aligned} \mathbf{Q}_{1,i} &= \mathbf{M}_i^1 + \tfrac{1}{11}(\mathbf{E}_i^1 + \mathbf{F}_i^1), \quad \mathbf{Q}_{10,i} = \mathbf{M}_i^3 - \tfrac{1}{11}(\mathbf{E}_i^3 + \mathbf{F}_i^3), \\ \mathbf{Q}_{i,1} &= \mathbf{M}_i^2 + \tfrac{1}{11}(\mathbf{E}_i^2 + \mathbf{F}_i^2), \quad \mathbf{Q}_{i,10} = \mathbf{M}_i^4 - \tfrac{1}{11}(\mathbf{E}_i^4 + \mathbf{F}_i^4). \end{aligned}$$

Thus the outermost control points and an array of control points adjacent to them have been determined. Fig. 4.1-(b),(e) show two arrays of control points along the quadrilateral.

Note that so far, the global compatible boundary condition related with the transverse tangent vectors $\mathbf{T}_i(t)$ $(i = 1, \cdots, 4)$ has been satisfied. Apart from these two arrays of control points along the quadrilateral, the rest of control points of the surface can be freely chosen, that means in fact there exists a family of surfaces interpolating the Bézier asymptotic quadrilateral constructed in Section 3. In order to get the rest of control points, one choice is by minimizing the thin plate spline energy of the surface as

$$\int_0^1 \int_0^1 (||\mathbf{R}_{uu}(u,v)||^2 + 2||\mathbf{R}_{uv}(u,v)||^2 + ||\mathbf{R}_{vv}(u,v)||^2) du dv. \tag{4.5}$$

In this way, we can acquire a fair interpolation surface. Fig. 4.1-(c),(f) show two pairs of Bézier surfaces interpolating the Bézier asymptotic quadrilaterals in Fig. 4.1-(a),(d).

Remark 4.1. Since we have already known two arrays of control points of surface, the Mask method [28] can be used reversely to determine the other free control points. There are four common masks, including the quasi-harmonic mask [29], Dirichlet mask [30], harmonic mask [31] and the bending mask [32]. Based on the data in Fig. 4.1-(b), the surface obtained by the harmonic mask is best (as shown in Fig. 4.2-(a)). However, this mask is not suitable for the data in Fig. 4.1-(e), since the resulting surface has self-intersecting curve (as shown in Fig. 4.2-(b)). Therefore, it's an efficient way to get the resulting surfaces by optimizing the thin plate spline energy.

5. Examples

Above analysis is trivial and is based on the condition that $\mathbf{r}_i''(t)$ never vanish. There may exist other cases like $\mathbf{r}_i''(t)$ is identically equal to zero and $\mathbf{r}_i''(t)$ vanishes for some parameter $t = t_0$, which are corresponding to line and curve with inflection. This section focuses on these two cases discussed by examples. We also argue the degree possibilities of boundary curves if satisfying the constraints.

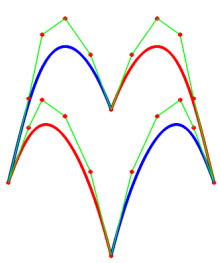

(a) The boundary asymptotic curves with their control points.

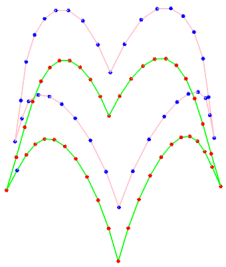

(b) Control points adjacent to the outermost.

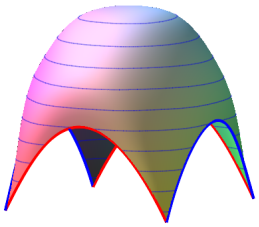

(c) The resulting Bézier Surface.

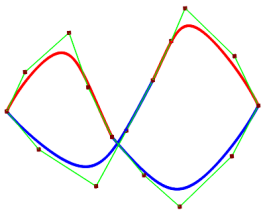

(d) The boundary asymptotic curves with their control points.

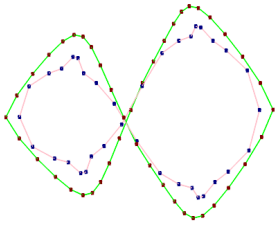

(e) Control points adjacent to the outermost.

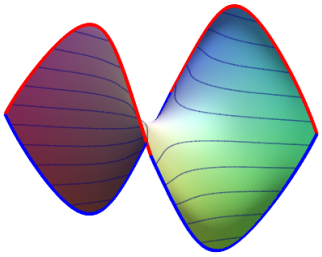

(f) The resulting Bézier Surface.

Fig. 4.1. Bézier surface interpolating the Bézier asymptotic quadrilateral.

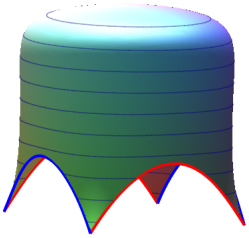

(a) Boundary data from Fig. 4.1-(b).

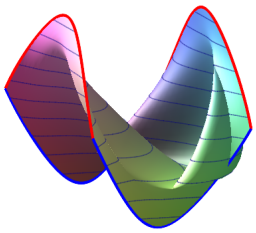

(b) Boundary data from Fig. 4.1-(e).

Fig. 4.2. Bézier surface obtained by the Mask method.

5.1. Boundary curves with lines

A special condition of the lamellas as shown in Fig. 1.1 are with straight strips, which means the asymptotic curves are mapped to straight lines on these developable strips. Thus, it's possible that the curves are just lines. According to Lemma 2.1, a line on the surface is also an asymptotic curve of it. Therefore we take quadrilateral with lines into consideration. The following examples discuss the condition when lines are parts of the boundary curves. The construction of the resulting Bézier surface is based on the method presented in Section 4.

Example 5.1. Let $\mathbf{r}_1(t)$ be a line in the quadrilateral. The construction of the quintic Bézier asymptotic quadrilateral is based on the analysis in Section 3.2. But some conditions should be modified to be compatible with the construction process. For condition (C1), $k_1(0) = 0$, $k_1(1) =$

0 and $\lambda_{13} = 0$, $\mu_{12} = 0$. For condition (C3), $\tau_2(0) = 0$, $\tau_4(0) = 0$. Also the definition of the tangent vector $\mathbf{T}_1(t)$ is changed as

$$\mathbf{T}_1(t) = x_1(t)\mathbf{r}_1'(t) + y_1(t)\mathbf{r}_2'(t) + z_1(t)\mathbf{r}_4'(1-t),\ t \in [0,1], \tag{5.1}$$

where

$$x_1(t) = \sum_{j=0}^{7} \alpha_{1j} B_j^7(t), \quad y_1(t) = \sum_{j=0}^{7} \beta_{1j} B_j^7(t), \quad z_1(t) = \sum_{j=0}^{7} \delta_{1j} B_j^7(t).$$

Its Bézier form is

$$\mathbf{T}_1(t) = 5 \sum_{j}^{11} \sum_{i=\max(0,j-4)}^{\min(7,j)} \frac{\binom{7}{i}\binom{4}{j-i}}{\binom{11}{j}} (\alpha_{1i} \cdot \Delta\mathbf{P}_{1,j-i} + \beta_{1i}\Delta\mathbf{P}_{2,j-i} + \delta_{1i}\Delta\mathbf{P}_{4,5+i-j}).$$

Some values of α_{1j}, β_{1j}, δ_{1j} $(j = 0, \ldots, 7)$ can be obtained, but the others are freely chosen. Similar to the construction of surface in Section 4, we can get two Bézier surfaces interpolating the Bézier asymptotic quadrilaterals with one line, which are shown in Fig. 5.1.

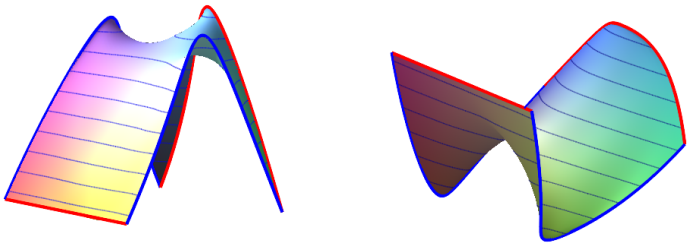

(a) One linear boundary. (b) One linear boundary.

Fig. 5.1. Bézier surface interpolating the Bézier asymptotic quadrilateral with one line.

Example 5.2. There are two geometric positions of two of boundary curves being lines, one is intersecting at the corner and the other is opposite. We discuss them below separately.

- Two intersecting lines.

  We assume $\mathbf{r}_1$, $\mathbf{r}_2$ are lines. Similar to the conditions related with $\mathbf{r}_1$ in Example 5.1, the conditions related with $\mathbf{r}_2$ are set as $k_2(0) = 0$, $k_2(1) = 0$, $\lambda_{22} = 0$, $\mu_{23} = 0$, $\tau_3(0) = 0$, $\tau_4(0) = 0$, and

  $$\mathbf{T}_2(t) = x_2(t)\mathbf{r}_2'(t) + y_2(t)\mathbf{r}_1'(t) + z_2(t)\mathbf{r}_3'(1-t), \tag{5.2}$$

  where

  $$x_2(t) = \sum_{j=0}^{7} \alpha_{2j} B_j^7(t), \quad y_2(t) = \sum_{j=0}^{7} \beta_{2j} B_j^7(t), \quad z_2(t) = \sum_{j=0}^{7} \delta_{2j} B_j^7(t).$$

- Two opposite lines.

Suppose $\mathbf{r}_1$, $\mathbf{r}_3$ are lines. Similarly, $k_3(0) = 0$, $k_3(1) = 0$, $\lambda_{32} = 0$, $\mu_{33} = 0$, $\tau_2(0) = 0$, $\tau_2(1) = 0$, $\tau_4(0) = 0$, $\tau_4(1) = 0$, and

$$\mathbf{T}_3(t) = x_3(t)\mathbf{r}_3'(t) + y_3(t)\mathbf{r}_2'(1-t) + z_3(t)\mathbf{r}_4'(t), \tag{5.3}$$

where

$$x_3(t) = \sum_{j=0}^{7} \alpha_{3j} B_j^7(t), \quad y_3(t) = \sum_{j=0}^{7} \beta_{3j} B_j^7(t), \quad z_3(t) = \sum_{j=0}^{7} \delta_{3j} B_j^7(t).$$

Fig. 5.2 illustrates four Bézier surfaces interpolating the Bézier asymptotic quadrilaterals with two lines.

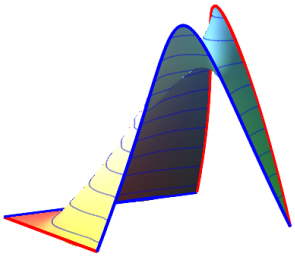

(a) Two linearly intersecting boundaries.

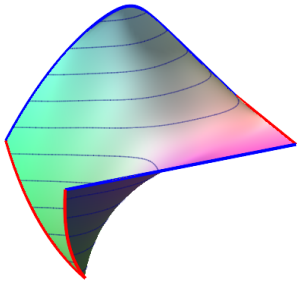

(b) Two linearly intersecting boundaries.

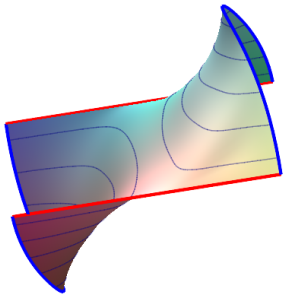

(c) Two linearly opposite boundaries.

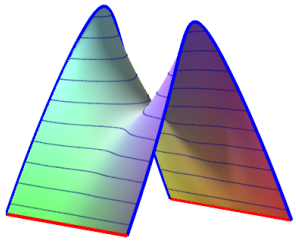

(d) Two linearly opposite boundaries.

Fig. 5.2. Bézier surface interpolating the Bézier asymptotic quadrilateral with two lines.

Example 5.3. Let $\mathbf{r}_i$ be lines and $k_i(j) = 0$ $(i = 1, 2, 3,\ j = 0, 1)$, $\lambda_{13} = 0$, $\mu_{12} = 0$, $\lambda_{22} = 0$, $\mu_{23} = 0$, $\lambda_{32} = 0$, $\mu_{33} = 0$, $\tau_4(0) = 0$, $\tau_4(1) = 0$, and $\mathbf{T}_i(t)$ $(i = 1, 2, 3)$ be represented in the form as (5.1), (5.2), (5.3). Fig. 5.3 exhibits two Bézier surfaces interpolating the Bézier asymptotic quadrilateral with three lines.

Example 5.4. It's a special case when four boundary curves are all linear. We can similarly model this kind of surfaces based on above analysis as shown in Fig. 5.4. In fact, it's not hard to identify that the resulting surface can only be either plane or hyperbolic paraboloid depending on whether the quadrilateral coplanar or not.

5.2. Boundary curves with inflection points

If there exists an inflection of curve $\mathbf{r}(t)$ at the point t_0, then $\mathbf{r}'(t_0) \times \mathbf{r}''(t_0) = 0$, and the left and right limits $\mathbf{b}_-$ and $\mathbf{b}_+$ of the binormal vectors are of opposite sign. When each of

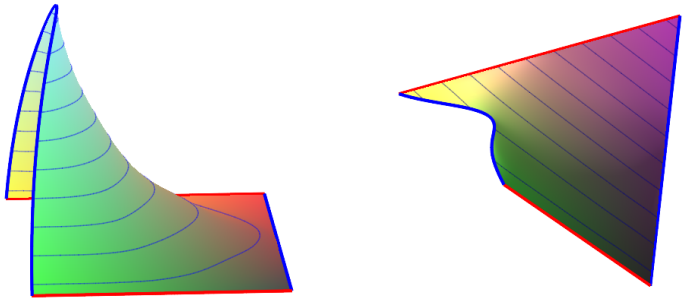

(a) Three linear boundaries. (b) Three linear boundaries.

Fig. 5.3. Bézier surface interpolating the Bézier asymptotic quadrilateral with three lines.

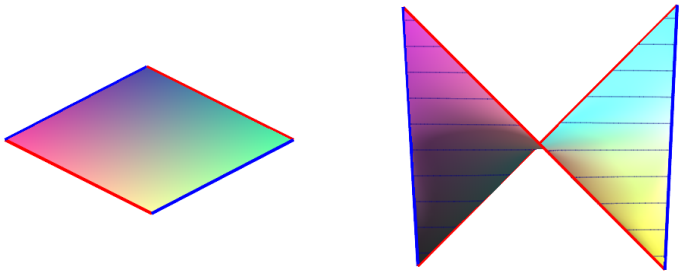

(a) Plane. (b) Hyperbolic paraboloid.

Fig. 5.4. Bézier surface interpolating the Bézier asymptotic quadrilateral with four lines.

the boundary curves $\mathbf{r}_i(t)$ $(i = 1, \ldots, 4)$ has one or two inflections, then the total number of reversals of the binormal vectors $\mathbf{b}(t)$ along the boundary curves is still even, which satisfies the constraint $(C3)$. Besides, on the premise that the constraint $(C1)$ and $(C2)$ are satisfied, we can construct Bézier surface interpolating the quintic Bézier asymptotic quadrilateral with inflections by the method presented in the following examples.

Example 5.5. We set the boundary curves $\mathbf{r}_i(t)$ $(i = 1, \ldots, 4,)$ are orthogonal at four corner points and each of them is a quintic Bézier curve with only one inflection point. The tangent vector $\mathbf{T}_i(t)$ vanishes at the inflection point with a reversal of direction. The Bézier surface interpolates the Bézier asymptotic quadrilateral with inflections as shown in Fig. 5.5.

(a) Each boundary curve with one infection. (b) Resulting surface

Fig. 5.5. Bézier surface interpolating the Bézier asymptotic quadrilateral with inflections.

Example 5.6. Fig. 5.6 shows that each curve of $\mathbf{r}_i(t)$ $(i = 1, \ldots, 4,)$ is a quintic Bézier curve with two inflection points.

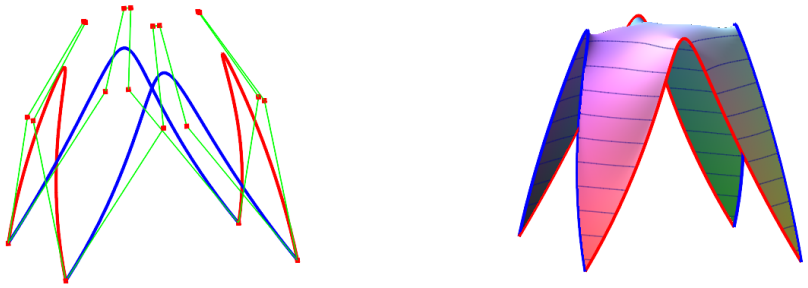

(a) Each boundary curve with two infections. (b) Resulting surface

Fig. 5.6. Bézier surface interpolating the Bézier asymptotic quadrilateral with inflections.

5.3. Degrees discussion

From what we have discussed before, we know that for the quintic Bézier boundary quadrilateral with given corner data, after construction under the local corner constraints, there are still free parameters left. This provides freedom to get asymptotic quadrilateral and minimizing the strain energy can help us get a smooth one. If the degree of the boundary curves is higher than five, then more free parameters can be freely chosen. Such condition suits for the construction of asymptotic quadrilateral with more restraints from the practical application.

If we want to reduce the degree of the boundary curve $\mathbf{r}_i$, we need to consider how many parameters are related, and the most important, how many parameters are free. For the quintic Bézier boundary curves, there are four free parameters left. So if we relax the given corner data, for example, the curvatures of the quadrilateral are not given in advance, then there will be 8 more free parameters. Thus, the number of control points on each boundary can be reduced to five so that the degree of boundary curve $\mathbf{r}_i$ is reduced to quartic. In a similarly constructed method, at last we find that there is one free parameter (about the initial curvature such as $k_1(0)$) left. Choosing $k_1(0)$ can help us construct asymptotic quadrilateral as we wish. And the strain energy is much easier: it's a quadratic function about $k_1(0)$. As discussed before, we can then use Bézier surface of bi-eight to interpolate this quartic asymptotic quadrilateral. In fact, this is a special case studied in [25] when all weights to be equal.

This analysis illustrates that decreasing the given information of the corner data can help us reduce the degree of the boundary curves. But less information will lead to the difficulty to solve function and what's worse it may have no solutions. So, here we just use the quintic Bézier boundary condition with given positions, tangents and curvatures to construct asymptotic quadrilateral. If insisted on lower degree with same boundary conditions, then cubic B-spline asymptotic quadrilateral is a good choice which can be interpolated by B-spline surface of bi-quintic degree (see [24]).

6. Conclusions and Future Work

Inspired by the application potentials of asymptotic curves in real architecture, we abstract a local geometry problem how to construct a surface interpolating curves as its asymptotic

boundary curves. We analyze the conditions to construct asymptotic quadrilateral and model Bézier surfaces interpolating quintic Bézier asymptotic quadrilateral. The construction of the resulting tensor-product Bézier surface satisfies the global compatible constraints along boundaries related with the transverse tangent vectors. The existing freedom to obtain both boundary quadrilateral and interpolated surface makes the construction flexible. In addition, the construction of surfaces interpolating asymptotic quadrilaterals with lines or inflections are also discussed by examples.

Using this method, we can easily fill in all the quads in Fig. 1.1 with smooth surfaces bounded by these asymptotic curves. However, how to make all the surfaces smooth globally along the asymptotic curves is not an easy and obvious generalization. This problem concerns patches joining and compatibility. A careful study of surfaces interpolation along a common asymptotic curve and an asymptotic vertex star is left for future research.

Acknowledgments. The authors are grateful to the reviewers for their helpful comments and suggestions. This work is partly supported by the National Natural Science Foundation of China (Nos. 11671068, 11271060, 11401077).

References

[1] G. Contopoulos, Asymptotic curve and escapes in Hamiltonian systems, *Astronomy and Astrophysics*, **231** (1990), 41-55.

[2] S.B. Angenent and J.J.L. Velázquez, Asymptotic shape of cusp singularities in curve shortening, *Duke Mathematical Journal*, **77**:1 (2013), 71-110.

[3] H.J. Wang and Q. Ni, A new method of moving asymptotes for large-scale unconstrained optimization, *Applied Mathematics and Computation*, **203** (2008), 62-71.

[4] S. Flöry and H. Pottmann, Ruled surfaces for rationalization and design in architecture, in *Proceedings of the 30th Annual Conference of the Association for Computer Aided Design in Architecture*, A. Sprecher et al. (ed.), ACADIA, America, 2010, 103-109.

[5] H. Pottmann, M. Eigensatz, A. Vaxman, and J. Wallner, Architectural geometry, *Computers and Graphics*, **47**:6 (2015), 215-216.

[6] E. Schling, D. Hitrec and R. Barthel, Designing grid structures using asymptotic curve networks, in *Humanizing Digital Reality*, K. De Rycke et al. (ed.), Springer, Singapore, 2018, 125-140.

[7] M.R. Jimenez, C. Müller, and H. Pottmann, Discretizations of surfaces with constant ratio of principal curvatures, *Discrete and Computational Geometry*, (2018), in press.

[8] A.I. Bobenko and Y.B. Suris, *Discrete Differential Geometry, Integrable Structure, Graduate Studies in Mathematics*, American Mathematical Society, Provindence, 2008.

[9] E. Schling, M. Kilian, H. Wang, J. Schikore, and H. Pottmann, Design and construction of curved support structures with repetitive parameters, *Advances in Architectural Geometry*, (2018), in press.

[10] G.J. Wang, K. Tang, and C.L. Tai, Parametric representation of a surface pencil with a common spatial geodesic, *Computer-Aided Design*, **36**:5 (2004), 447-459.

[11] C.Y. Li, R.H. Wang, and C.G. Zhu, Parametric representation of a surface pencil with a common line of curvature, *Computer-Aided Design*, **43** (2011), 1110-1117.

[12] E. Kasap, F.T. Akyyildiz, and K. Orbay, A generalization of surface family with common spatial geodesic, *Applied Mathematics and Computation*, **201** (2008), 781-9.

[13] C.Y. Li, R.H. Wang, and C.G. Zhu, A generalization of surface family with common line of curvature, *Applied Mathematics and Computation*, **219** (2013), 9500-9507.

[14] C.Y. Li, R.H. Wang, and C.G. Zhu, Design and G^1 connection of developable surface through Bézier geodesics, *Applied Mathematics and Computation*, **218** (2011), 3199-3208.

[15] C.Y. Li, R.H. Wang, and C.G. Zhu, An approach for designing a developable surface through a given line of curvature, *Computer-Aided Design*, **45** (2013), 621-627.

[16] R.T. Farouki, N. Szafran, and L. Biard, Existence conditions for Coons patches interpolating geodesic boundary curves, *Computer Aided Geometric Design*, **26** (2009), 599-614.

[17] L. Biard, R.T. Farouki, and N. Szafran, Construction of rational surface patches bounded by lines of curvature, *Computer Aided Geometric Design*, **27** (2010), 359-371.

[18] R.T. Farouki, N. Szafran, and L. Biard, Construction and smoothing of triangular Coons patches with geodesic boundary curves, *Computer Aided Geometric* Design, **27** (2010), 301-312.

[19] R.T. Farouki, N. Szafran, and L. Biard, Construction of Bézier surface patches with Bézier curves as geodesic boundaries, *Computer-Aided Design*, **41** (2009), 772-781.

[20] H.G. Yang and G.Z. Wang, Optimized design of Bézier surface through Bézier geodesic quadrilateral, *Journal of Computational and Applied Mathematics*, **273** (2015), 264-273.

[21] H.G. Yang and G.Z. Wang, Construction of B-spline surface with B-spline curves as boundary geodesic quadrilateral, *Journal of Computational and Applied Mathematics*, **290** (2015), 104-113.

[22] E. Bayram, F. Güler, and E. Kasap, Parametric representation of a surface pencil with a common asymptotic curve, *Computer-Aided Design*, **44** (2012), 637-643.

[23] G.S. Atalay, and E. Kasap, Surfaces family with common null asymptotic, *Applied Mathematics and Computation*, **260** (2015), 135-139.

[24] H. Wang, C.G. Zhu, and C.Y. Li, Construction of B-spline surface from cubic B-spline asymptotic quadrilateral, *Journal of Advanced Mechanical Design, Systems, and Manufacturing*, **11**:4 (2017), JAMDSM0044.

[25] H. Wang, C.G. Zhu, and C.Y. Li, Construction of rational Bézier surface interpolating asymptotic quadrilateral, *Journal of Computer-Aided Design and Computer Graphics*, **29**:8 (2017), 1497-1504.

[26] M.P. Do Carmo, *Differential Geometry of Curve and Surface*, Prentice Hall, Englewood Cliffs, 1976.

[27] G. Farin, *Curves and Surfaces for CAGD: A Practical Guide*, 5th edition, Morgan Kaufmann, San Francisco, 2002.

[28] G. Farin and D. Hansford, Discrete Coons patches, *Computer Aided Geometric Design*, **16**:7 (1993), 691-700.

[29] D.L. Chopp, Computing minimal surfaces via level set curvature flow, *Journal of Computational Physics*, **106** (1993), 77-91.

[30] J. Monterde, Bézier surfaces of minimal area: Dirichlet approach, *Computer Aided Geometric Design*, **21**:2 (2004), 117-136.

[31] J. Monterde and H. Ugail, On harmonic and biharmonic Bézier surfaces, *Computer Aided Geometric Design*, **7** (2004), 697-715.

[32] Y. Miao, H. Shou, J. Feng, Q. Peng, and A.R. Forrest, Bézier surfaces of minimal internal energy, in *Mathematics of Surfaces XI, Lecture Notes in Computer Science*, Springer, Germany, 2005, 318-335.